

STRUCTURAL, OPTICAL AND MORPHOLOGICAL INVESTIGATIONS OF Fe-DOPED SnS THIN FILMS

V. JANAKIRAMAN^{a,*}, V. TAMILNAYAGAM^b, R. S. SUNDARARAJAN^a,
S. SIVABALAN^c, B. SATHYASEELAN^d

^a*PG & Research Department of Physics, Government Arts College (Autonomous) (Affiliated to Bharathidasan University), Kumbakonam, Tamilnadu 612002, India*

^b*Department of Physics, A.P.A. College of Arts & Culture, Palani, Dindigul, Tamilnadu, India*

^c*Department of Physics, T.B.M.L. College, Porayar 609307, Tamilnadu, India*

^d*Department of Physics, University College of Engineering Arni (A Constituent College of Anna University Chennai) Arni 632326, Tamil Nadu, India*

SnS could have novel applications in optoelectronics including solar cell devices, sensors, batteries and also in biomedical sciences. Fe-doped SnS thin films were prepared on glass substrates using chemical spray pyrolysis (CSP) method. Pure and Fe-doped SnS thin films were deposited onto microscopic glass substrates using the spray pyrolysis technique. The precursors of SnCl₂·2H₂O (0.1 M) and thiourea (0.1 M) were dissolved separately in a solution containing deionised water and isopropyl alcohol in proper ratio. Equal volumes of these two solutions were mixed together and sprayed onto the microscopic glass substrates at a substrate temperature of 450^oC. Fe was doped with SnS thin films using FeCl₃ (5 at.%, 7 at.%, 9 at.%, and 11 at.%) as the dopant source. Structural, optical, vibrational, structural, morphological properties were studied.

(Received April 18, 2020; Accepted August 10, 2020)

Keywords: Fe-Doped SnS Thin Films, Spray pyrolysis, Band gap, Gas sensors

1. Introduction

Since low cost, non-toxic, and good abundance in nature, tin (II) sulphide (SnS) is a candidate for next-generation multifunctional devices. SnS could have novel applications in optoelectronics including solar cell devices, sensors, batteries, and also in biomedical sciences [1-3]. SnS is one of the tin chalcogenide layered semiconductors in group IV–VI with orthorhombic crystal structure, and exhibits p-type electrical conduction. Since SnS has high optical absorption ($\alpha > 10^4 \text{ cm}^{-1}$) above the direct absorption edge at 1.3–1.5 eV, it is one of the most promising absorber materials for solar cells [4,5]. The SnS films can be prepared by variety of techniques such as vacuum evaporation [6], chemical bath deposition [7], RF-sputtering [8], dip deposition [9] and chemical spray pyrolysis [10]. Among these, chemical spray pyrolysis is one of the simplest and cost effective means of thin film deposition. Hence, this technique was selected for the deposition of SnS thin films in the present work. The enhancement of the solar cell efficiency can be done by adding doping elements into the SnS layer [11]. In this article, Fe-doped SnS thin films were prepared on glass substrates using chemical spray pyrolysis (CSP) method. Optical, vibrational, structural, and surface morphological properties of Fe-doped SnS thin films have also been reported.

* Corresponding authors: v.raman.in@gmail.com

2. Experimental details

Pure and Fe-doped SnS thin films were deposited onto microscopic glass substrates using the spray pyrolysis technique. The precursors of $\text{SnCl}_2 \cdot 2\text{H}_2\text{O}$ (0.1 M) and thiourea (0.1 M) were dissolved separately in a solution containing deionised water and isopropyl alcohol in proper ratio. Equal volumes of these two solutions were mixed together and sprayed onto the microscopic glass substrates at a substrate temperature of 450°C . Fe was doped with SnS thin films using FeCl_3 (5 at.%, 7 at.%, 9 at.%, and 11 at.%) as the dopant source. The substrates were first cleaned with a water bath, followed by dipping in concentrated HCl, acetone and ethanol successively. Finally the substrates were rinsed in deionized water and allowed to dry in a hot air oven. In spray unit, the substrate temperature was maintained with the help of heater, controlled by a feedback circuit. During spray, the substrate temperature was kept constant. Spray head and substrate heater kept inside a chamber, provided with an exhaust fan for removing gaseous by-products and vapors from the solvent. The values of deposition parameters like solution flow rate, carrier gas pressure and nozzle to substrate distance were kept as 2 ml/min, 1.5 bar and 20 cm, respectively. A uniform coating on the substrate is achieved. Following deposition, the film was allowed to cool slowly to room temperature and washed with distilled water and then dried.

3. Characterization

Powder X ray diffraction was observed for the sample by Rigaku III model. Fourier transform infrared spectra were recorded by the KBr pellet technique using a Bruker 66 V FTIR spectrometer to confirm the presence of functional group in the sample with scanning range of wave number $400\text{--}4000\text{ cm}^{-1}$. UV-Vis spectrum was recorded in the range of $200\text{--}2000\text{ nm}$ using VARIAN CARY 5E spectrometer. The surface morphology and elemental analysis were studied using TESCAN SEM-VEGA III and CONTEXT softwares respectively.

4. Results and discussion

4.1. Powder XRD Analysis

Figure 1 shows the X-ray diffraction (XRD) spectra for as-deposited and Fe doped SnS thin films at deposited at (0%, 5%, 7%, 9% and 11%) concentrations at 450°C . Broad reflectance of XRD peaks of as prepared thin films can be attributed to a small grain size of the particles. A peak appear at 26.48° , 33.83° , 37.73° and 51.71° , which could be assigned to (111), (220), (131) and (311) planes. The diffraction peaks are recognized to SnS taken from the Joint Committee of Powder Diffraction Standard (JCPDS: 39-0354) [12].

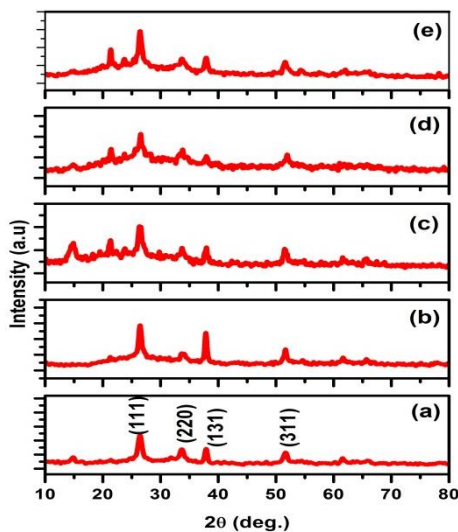


Fig. 1. X-ray diffractogram of pure SnS and Fe-doped SnS and thin films (a) pure SnS (b) 5%, (c) 7%, (d) 9%, and (e) 11%.

This indicates that the particles are SnS with a strong (111) reflection plane. The favored location of the particle is due to the circumstance that the growing method is controlled by nucleation. The results are in agreement with the finding of reported researches [13-15]. The crystallite size was calculated from Scherer's equation [16]

$$D = 0.9\lambda / \beta \cos\theta \quad (1)$$

where λ is the X-ray wavelength (\AA), β is the full width at half maximum intensity (FWHM) (radian), θ is Bragg's diffraction angle of the XRD peak (degree). The pure SnS sample has a particle size of 18.6 nm, 5% Fe-doped SnS thin films particle size is 16.34 nm, 7% Fe-doped SnS thin film at the particle size 15.69 nm. Similarly for 9% which has particle size 14.2 nm. But when doping at 11%, it has merely 12 nm. Hence the doping percentage increases particle size decreases. This result predicts the uniformity among the dopants and shows the ability for sensing purpose. The reason is more dopant atoms occupy the tin lattice sites resulting more charge carriers. The uniformity in result consistency delivers the fruitful applications for renewable energy source like solar cells [17, 18].

4.2. UV analysis

The optical transmittance and absorbance spectra for undoped and Fe-doped SnS films deposited at 450°C under different concentrations are shown in Fig. 2. It was observed at different cutoff wavelengths with very good absorbance and transmittance properties. Undoped SnS film has different peaks at 327 nm, 333 nm, 348 nm, 353 nm, 374 nm and 390 nm for its absorbance, whereas transmittance value increases beyond 500 nm in UV-Vis-Near IR regions. This shows the gradual increase of transparency with increasing wavelength. The Fe-doped SnS film with 5, 7, 9, 11 percentage of doping results absorbance value at 305 nm, 318 nm, 363 nm, 333 nm, respectively. The gradual increase in the absorbance cutoff wavelength shows the interstitiality of atom arrangements with regularity. But at 11% doping the cutoff absorbance value decreases shortly. This shows the increase in transparency for that particular amount of dopants. Similarly for 5, 7, 9, 11% of Fe-doped SnS films the transparency point values increases at 300 nm itself when compared to undoped film. The maximum transparency got from at 5% of Fe-doped SnS thin film. So it is advisable that the iron atoms must be doped below 5% or above 10% are the expected dopants for good transparency films.

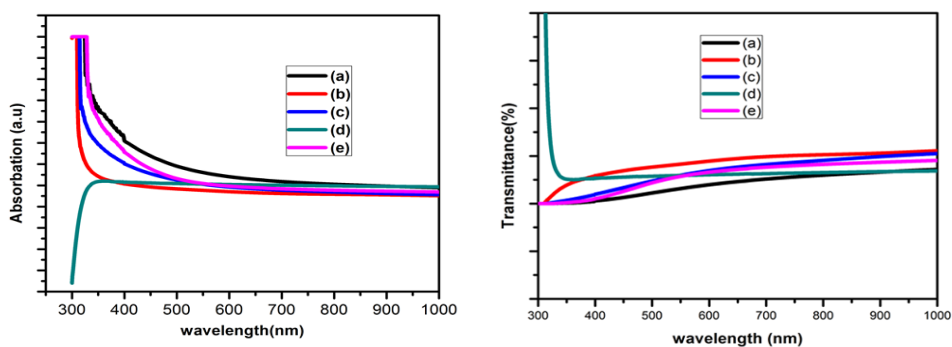


Fig. 2. Absorbance and transmittance spectra of pure SnS and Fe-doped SnS thin films (a) pure SnS (b) 5%, (c) 7%, (d) 9%, and (e) 11%.

4.3. FTIR analysis

The functional group analysis for Fe doped SnS thin film (5%) shows various vibrational assignment modes. According to Fig. 3a peaks at 1914 cm^{-1} and 1789 cm^{-1} represents the presence of metal carbonyl compounds. Peak at 1620 cm^{-1} confirms the presence of Fermi resonance overtone (NH₂). Peak 1325 cm^{-1} confirms the presence of CH-bending mode whereas peak at 1240.7 cm^{-1} represents CH₂ wagging. Peak at 1126 cm^{-1} confirms the presence of sulphate molecules and inorganic compounds. Peaks at 863 cm^{-1} , 824 cm^{-1} , 753 cm^{-1} , 715 cm^{-1} , represents the strong broad NH₂ wagging functional groups. Peaks at Fe doped SnS thin film (7%) 1917 cm^{-1} represents the presence of metal carbonyl compounds and 1813 cm^{-1} confirms the presence of Fe. Peak at 1389 cm^{-1} represents the potassium nitrate impurity in salts such as KBr due to CH₃ symmetric deformation. Peak at 1207 cm^{-1} is due to the presence of the inorganic tin-CH₃ group with medium assignment. Similarly 1001 cm^{-1} peak represents the inorganic sulphate present in the compound. According to Fig. 3c peak at 2302 cm^{-1} represent the presence of nitrogen atoms and the presence of Sn-H bonding. Peak at 1797 cm^{-1} represents the presence of Fe. 1234 cm^{-1} peak represents the presence of sulphate group. Peaks at 897 cm^{-1} and 428 cm^{-1} indicates N-N and Iron oxide molecules respectively. According to Fig. 3d iron and tin atoms indicates the peak at 1797 cm^{-1} . Peaks at 1384 cm^{-1} and 1342 cm^{-1} represents O-CH₂ wagging. Peaks at 755 , 716 , 672 , 642 , 582 cm^{-1} represent the presence of tin oxide. The undoped SnS thin films (Fig. 3e) having peaks at 585 , 643 , and 670 cm^{-1} confirms Sn-C presence. Peak at 1799.92 cm^{-1} represents the Fe-Sn atoms. Similarly peak at 1158 cm^{-1} represents the presence of sulphide [10, 13].

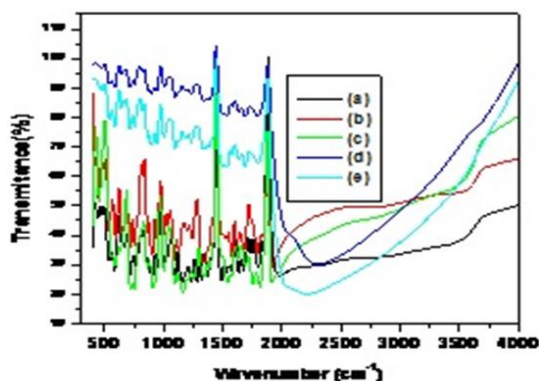


Fig. 3. FTIR spectra of pure SnS and Fe-doped SnS thin films (a) pure SnS (b) 5%, (c) 7%, (d) 9%, and (e) 11%.

4.4. Morphological analysis

The morphological properties of undoped and Fe doped SnS thin film are as shown in Fig. 4a–e. The undoped SnS thin film has smooth and regular growth of nucleation. Fe-doped SnS thin film (5%) represents the morphology as rough and aggregated grains in structure. This is due to the presence of iron atoms in tin molecular substrate. For 7% doping the surface is like nanostructured film with nano spaghetti behavior. For 9% Fe-doped SnS thin film, nanostructured fine grains having dendrite growth with agglomeration dendrites in some areas is found. On Fe-doped SnS thin film prepared by spray pyrolysis technique is varying from different dimensions as per observations. It can be well controlled through deposition parameters showing irregularity grains and dimensional heterogeneous particle size. From this it is clear that under different particle dimensions, there may be some possibility for sensing and storage like applications by using these selected structured grained films after the proper synthesis of the materials.

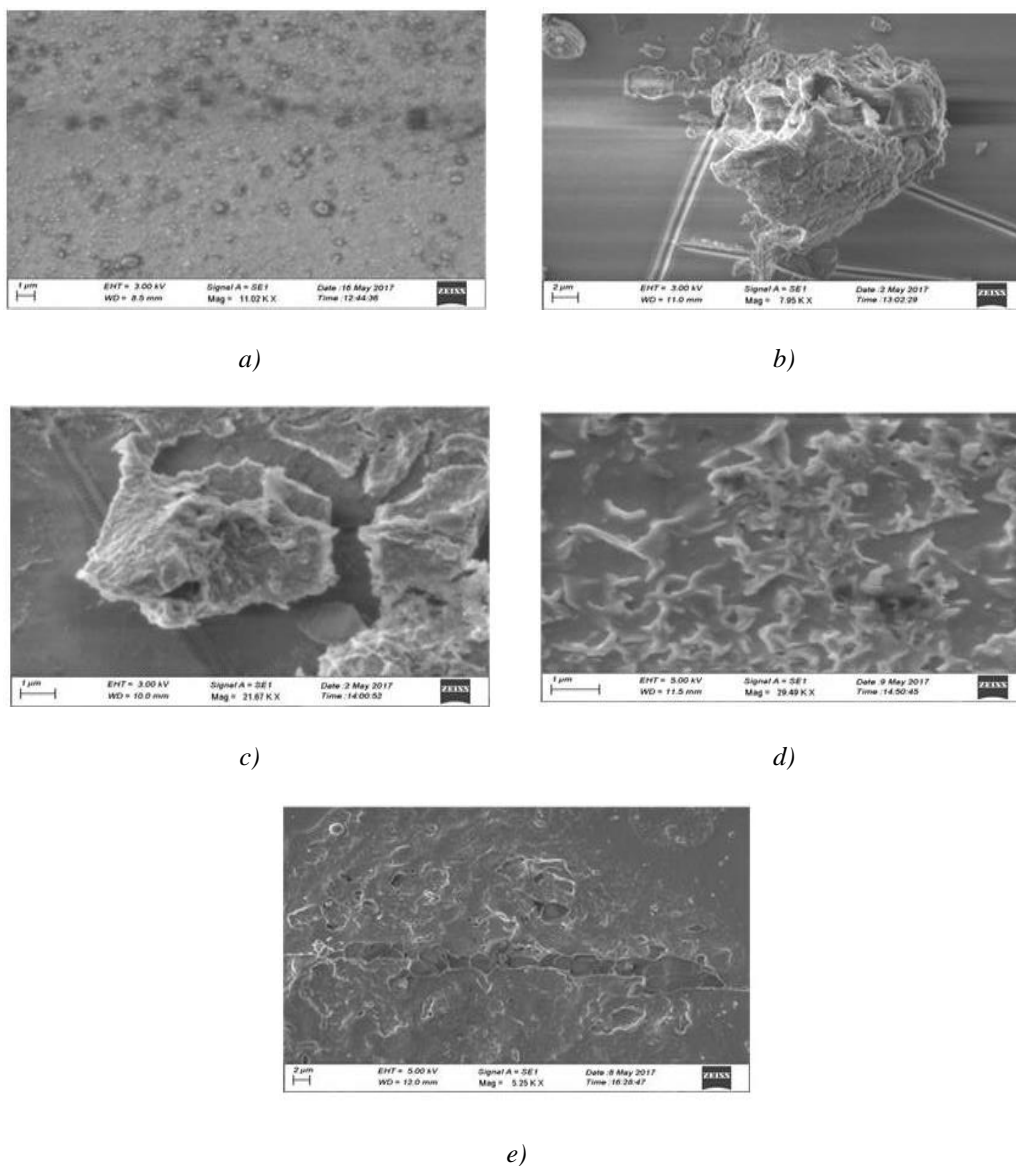


Fig. 4. SEM micrographs of of pure SnS and Fe-doped SnS and thin films (a) pure SnS (b) 5%, (c) 7%, (d) 9% and (e) 11%.

5. Conclusions

In this work pure and Fe doped SnS thin films were prepared using chemical spray pyrolysis method. Fe was doped with SnS thin films at different percentages (5 at.%, 7 at.%, 9 at.%, and 11 at.%). Structural, optical, vibrational, morphological properties of pure and Fe-doped SnS thin films were studied. Fe-doping incorporation into SnS thin film has been confirmed by XRD analysis, which proves the fruitful applications for renewable energy source like solar cells and ability for sensing purpose.

From UV analysis there is a gradual increase in the absorbance cutoff wavelength proves the interstitiality of atom arrangements with regularity. The maximum transparency got from at 5% of Fe-doped SnS thin film. FTIR analysis confirms the presence of Fe dopants incorporated in SnS film matrix. From SEM studies it is observed that Fe-doped SnS thin film is varying from different dimensions. It can be well controlled through deposition parameters. Hence, Fe doped SnS is a promising material for solar cells and gas sensors.

References

- [1] N. Koteeswara Reddy, M. Devika, E. S. R. Gopal, *Critical Reviews in Solid State and Materials Sciences* **40**(6), 359 (2015).
- [2] D. Avallaneda, G. Delgado, M. T. S. Nair, P.K. Nair, *Thin Solid Films* **515**, 5771 (2007).
- [3] M. Messaoudi, M. S. Aida, N. Attaf, S. Satta, *Chalcogenide Lett* **16**(4) 157—162 (2019)
- [4] M. Parenteau, C. Carlone, *Phys. Rev. B Condens. Matter* **41**, 5227 (1990).
- [5] R. D. Engelken, H. E. Mc Cloud, C. Lee, M. Slayton, H. Ghoreishi, *J. Electrochem. Soc.* **134**, 2696 (1987).
- [6] L. Price, I. P. Parkin, A. M. E. Hardy, R. J. H. Clark, *Chem. Mater* **11**, 1792 (1999).
- [7] A. Akkari, C. Guasch, N. Kamoun-Turki, *J. Alloys Compd.* **490**, 180 (2010).
- [8] W. Guang-Pu, Z. Zhi-Lin, Z. Wei-Ming, G. Xiang-Hong, C. Wei-Qun, H. Tanamura, M. Yamaguchi, H. Noguchi, T. Nagatomo, O. Omoto, *Proceedings of the First World Conference on Photovoltaic Energy Conversion, Hawaii, USA*, 365 (1994)
- [9] S. C. Ray, M. K. Karanjai, D. D. Gupta, *Thin Solid Films* **350**, 72 (1999).
- [10] K. Santhosh Kumar, C. Manoharan, S. Dhanapandian, A. Gowri Manohari, *Spectrochimica Acta Part A: Molecular and Biomolecular Spectroscopy* **115**, 840 (2013).
- [11] L. Chinnappa, K. Ravichandran, B. Sakthivel *Proc Indian Natn Sci Acad* **79**(3), 409 (2013).
- [12] JCPDS, Joint Committee for Powder Diffraction Standards, *Power Diffraction File for Inorganic Materials*, 39-0354, (1979).
- [13] H. Peng, L. Jiang, J. Huang, G. Li, *J. Nanoparticle Res.* **9**, 1163 (2007).
- [14] J. Henry, K. Mohanraj, S. Kannan, S. Barathan, G. Sivakumar, *Journal of Experimental Nanoscience* **10**(2), 78 (2015).
- [15] A. H. Bushra, H. S. Ikhlas, *J. of Nanotechnology & Advanced Materials* **2**(2), 43 (2014).
- [16] C. Gumus, O. M. Ozkendir, H. Kavak, Y. Ufuktepe, *J. Optoelectron. Adv. M.* **8**, 299 (2006).
- [17] Meriem Reghima, Anis Akkari, Cathy Guasch, Michel Castagné, Najoua Kamoun-Turki, *Journal of Renewable and Sustainable Energy* **5**, 063109 (2013).
- [18] Ninan, Rajeshmon, Sudha Kartha, Vijayakumar, *Solid State Physics, AIP Conf. Proc.* **1591**, 1440 (2014).